Biophysical Chemistry 266 (2020) 106453

Contents lists available at ScienceDirect

Biophysical Chemistry

journal homepage: www.elsevier.com/locate/biophyschem

Evidence of cadmium and mercury involvement in the Aβ42 aggregation process

Daniela Meleleo*, Cesare Sblano, Maria Maddalena Storelli, Rosanna Mallamaci

Department of Biosciences, Biotechnologies and Biopharmaceutics, University of Bari "Aldo Moro", via E. Orabona 4, 70126 Bari, Italy

HIGHLIGHTS

- Aβ42 toxicity increases significantly in the presence of either Cd^{2+} or Hg^{2+}.
- Cd^{2+} and Hg^{2+} reduce Aβ42's capacity to form ion channels characterized by neutral ion selectivity.
- Cd^{2+} and Hg^{2+} promote the formation of high-molecular-weight aggregates.

GRAPHICAL ABSTRACT

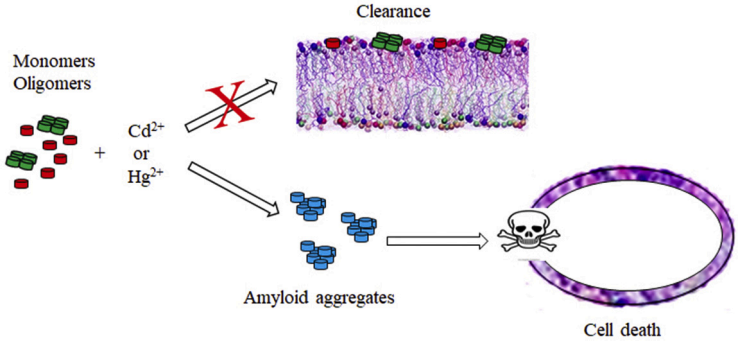

ARTICLE INFO

Keywords:
Cadmium
Mercury
Aβ42
Aggregation
Cytotoxicity

ABSTRACT

Aβ42 is a small peptide formed from 42 aminoacids that presents a great propensity to aggregate until it forms fibrils. Aβ42 aggregation and fibrillation are very complex processes whose molecular mechanisms seem to depend on characteristics intrinsic to the peptide molecule, as well as extrinsic factors. Peptide concentration, mean pH and several substances, including metal ions, are principal extrinsic factors for the oligomerization process. Different metals affect the aggregation of the Aβ42 molecule, and their toxicity favours the misfolding and aggregation of the peptide. In this study, we evaluate the effect of different concentrations of Cd^{2+} and Hg^{2+} on the Aβ42 peptide in solution by different methods. The toxicity of Aβ42 was evaluated with the MTT assay, while the aggregation process was monitored by single-channel measurements, electrophoresis and western blot. Cd^{2+} and Hg^{2+} seem to favour the formation of high-molecular-weight aggregates, to decrease ion channel turnover inside the membrane and to significantly increase Aβ42 toxicity.

1. Introduction

Aβ42 is a small peptide formed from 42 aminoacids that presents a great propensity to aggregate until it forms fibrils. The fibrils precipitate extracellularly, forming senile plaques that are typical hallmarks of Alzheimer's disease (AD). Aβ42 aggregation and fibrillation are very complex processes whose molecular mechanisms are the subject of intensive studies. They seem to depend on characteristics intrinsic to the peptide molecule, as well as extrinsic factors. Aβ42 peptide, which is involved in AD, shows a great tendency to aggregate and self-assemble, probably due to its amphiphilic character. Misfolded Aβ42 peptide aggregates, initiating from monomers, then form dimers,

* Corresponding author.
E-mail addresses: danielaaddolorata.meleleo@uniba.it (D. Meleleo), cesare.sblano@uniba.it (C. Sblano), mariamaddalena.storelli@uniba.it (M.M. Storelli), rosanna.mallamaci@uniba.it (R. Mallamaci).

https://doi.org/10.1016/j.bpc.2020.106453
Received 16 June 2020; Received in revised form 30 July 2020; Accepted 2 August 2020
Available online 08 August 2020

trimers, large oligomers, protofibrils and ultimately fibrils. Several studies have highlighted that oligomeric species are more toxic than fibrils. Indeed, senile plaques have often been detected in non-demented individuals [1–4], while – in comparison with controls – soluble oligomers have more often been found in AD patients' brains, where they are strongly correlated with disease severity [5–10]. The hypothesis proposed is that soluble oligomers play an important role in triggering the early events causing AD, while senile plaques, constituting a reservoir, contribute to neuronal injury [11].

Although the processes of Aβ42 oligomerization and fibrillation are spontaneous, numerous factors can influence it. Peptide concentration, mean pH, specific membrane lipids and several substances, including toxic gases and metal ions, are principal factors in the oligomerization and fibrillation processes [12–15]. Results from numerous studies have suggested that the binding of Aβ42, as well as of Aβ40, to specific membrane lipids plays a key role in promoting Aβ42 aggregation. The form of Aβ42 bound to a cluster of monosialoglanglioside (GM1) may serve as a seed for the formation of Aβ42 aggregates [16,17]. Using MD simulations, Cheng and colleagues have shown that beta amyloid fibrils bound to liquid-ordered domains or GM1 exhibit diversified membrane-bound conformations and may be operative in cell membranes [18]. These studies reinforce the concept that the aggregation of amyloid beta peptides (Aβs) also occurs in lipid rafts as well as in solution, contributing to clarify Aβs' mechanism of toxicity. On the other hand, transient and heterogeneous properties of Aβ monomers and oligomers together with their self-assembly propensity make it difficult to determine the structure experimentally; therefore, a combination of NMR techniques and atomistic molecular dynamic simulations have been used to determine their atomic structures [19,20]. The study carried out by Saranya et al. shows that Aβ42 interacts with toxic gases such as CO, CO_2, SO_2 and NO_2 to form complexes. Due to the high number of intramolecular hydrogen bonds and a reduced probability of α-helices in the complexes, interaction with toxic gases may enhance the toxicity and aggregation of Aβ42 [13]. Several studies have shown that different metals (calcium, iron, mercury, cadmium) affect the aggregation of Aβ42-misfolded molecules and their toxicity [21–23]. High concentrations of Ca^{2+} (40 μM), in the presence of unilamellar vesicles (LUVs) made up of total lipid brain extracts, increase both the fiber formation kinetics and the total amount of fiber of Aβ [24]. The study of the aggregation of amyloidogenic peptides (Aβs) in the presence of metal ions, by fluorimetry and Fourier transform infrared spectroscopy, shows that ions can promote the aggregation of Aβ42 and Aβ40. The aminoacid residues involved in binding with metal ions seem to be the histidine residues at positions 6,13,14 of the N-terminal end, as demonstrated by Raman spectroscopic analysis of senile plaques in the human Aβ sequence [25] and by NMR and EPR spectroscopic analysis in synthetic Aβs [26]. The results obtained by Minicozzi and colleagues indicate that the histidine residues (at the above positions) and the glycine residue at position 11 are involved in forming Aβ42 binding sites for Zn^{2+} in solubilised monomers [27]. A recent study carried out by Sahoo and colleagues shows that when the Aβ peptide is complexed with Zn^{2+}, insulin-degrading enzyme (IDE) and its mutant ($_{E111Q}$IDE) are not able to cleave Aβ40 monomers to small and nontoxic fragments due to the fact that the Zn-Aβ complex does not fit the catalytic cavity of IDE. These results highlight the crucial role of Zn^{2+} in the formation of aggregates that are resistant to enzymatic degradation by IDE [28]. Chen and colleagues have shown that fibril formation depends on the binding affinities of Zn^{2+}, Cu^{2+}, Fe^{3+} and Al^{3+} and that in the concentration range of 25–500 μM, the effect is stronger for Fe^{3+} and Al^{3+} [29]. The study carried out by Syme et Viles reported that, like Zn^{2+}, Cd^{2+} coordinates Aβ molecules in an inter-molecular manner, thus favouring the formation of high-molecular-weight polymer species [30]. The involvement of metal ions in the aggregation process is confirmed by results of studies with metal ion chelators that inhibit the aggregation of synthetic amyloid peptides [31–33]. Numerous compounds, both plant-derived and synthetic, such as flavonoids and aminoisoflavones, interact with metal ions, Aβs and metal ion-Aβ complexes due to their chelation properties and hydrophilic and hydrophobic interactions with Aβ [34,35]. Besides, the structures of small molecules designed to modulate the reactivities of metal-free and metal-bound Aβs, have been investigated using a multidisciplinary approach. The results of these studies show that while some small molecules diminish oxidative stress, others decrease the toxicity of metal-Aβs complexes and Aβs alone [36,37]. Finally, the study carried out by Zhang and colleagues indicates that the D3 peptide (consisting of 12 all-D-peptide residues), stabilizes Aβ42 monomers, to the disadvantage of its aggregation process [38].

Several studies demonstrate that metal ions increase the neurotoxicity of Aβs by different mechanisms, such as the membrane fragmentation by lipid loss due to fiber growth on the membrane surface [24], the induction of the release of Aβ peptides [39], Aβ accumulation through APP overproduction and reduction of neprilysin [40], the significant reduction in viability of SH-SY5Y cells [41], the formation of highly neurotoxic complexes [29,33,42,43] whose respective aggregates are associated with high neurotoxicity in neuroblastoma cell cultures [21]. These studies suggest a possible link between AD and metal ions, a concept reinforced by observations that the concentrations of several metals in plasma and cerebrospinal fluid (CSF) were significantly higher in subjects with AD than in control [44–46]. The results obtained by Gerhardsson and colleagues show that the medians and ranges of plasma concentrations (expressed as μg/l) of total mercury (inorganic Hg + organic Hg) and cadmium (Cd) in patients with AD/controls are 0.28 (< 0.21–2.1)/ < 0.21 (< 0.21–0.41) and 0.05 (< 0.04–0.34)/0.05 (< 0.04–0.27), respectively. Using the same records, the medians and ranges of CSF concentrations are < 0.21 (< 0.21–0.28)/ < 0.21 (< 0.21–0.30) and < 0.04 (< 0.04–0.15)/ < 0.04 (< 0.04–0.08), respectively [44]. Mutter and colleagues have described similar values of Hg concentration (2.64 μg/L) in the blood of patients with AD [45]. Indeed, Cd and Hg are two environmental contaminants with a well-described toxicology. The neurotoxic effects of cadmium and mercury are caused by both acute (≥100 μM and ≥ 200 μg/L, respectively) and chronic (0–40 μM and 0–35 μg/L, respectively) exposure [47–49].

In this study, we proposed to evaluate the effect of Cd^{2+} and Hg^{2+} different concentrations on the Aβ42 peptide in solution by different methods. To our knowledge, this is the first study to test the effect of Cd^{2+} and Hg^{2+} on the aggregation state of the Aβ42 peptide. The toxicity of Aβ42 was evaluated with the MTT assay, while the aggregation process was monitored by single-channel measurements, electrophoresis and western blot. We carried out experiments of cell viability in neuroblastoma cell cultures, of incorporation and channel formation into planar lipid membranes (PLMs) and of non-denaturing PAGE using metal ion-Aβ42 peptide mixtures.

2. Materials and methods

2.1. Chemicals

Aβ42 peptide, Cadmium chloride ($CdCl_2$), Mercury chloride ($HgCl_2$), Potassium chloride (KCl), and [3-(4,5-dimethylthiazol-2-yl)-2,5-diphenyl-tetrazolium bromide] (MTT) were purchased from Sigma (Germany).

2.2. Preparation of Aβ42 and heavy metals solutions

For the cell-viability and single-channel measurement experiments, a stock solution of Aβ42 was prepared by dissolving Aβ42 powder (0.1 mg) in 48 μL of bidistilled sterile water under stirring for 3 min to obtain a concentration of 4.6×10^{-4} M. From this solution, 5 μL were withdrawn and diluted in 45 μL of bidistilled sterile water under stirring for 3 min to obtain a concentration of 4.6×10^{-5} M. For the electrophoresis experiments, a stock solution of Aβ42 was prepared by

dissolving Aβ42 powder (0.1 mg) in 10 mM NaOH, sonicated in an ice bath for 5 min; the pH was then adjusted to 7.3 with phosphate buffer to obtain a concentration of 97.2×10^{-6} M in 10 mM phosphate. This protocol was used to disaggregate pre-seeded Aβ42 and obtain a monomeric peptide. The solutions were stored at −20 °C until use.

Stock solutions of $CdCl_2$ or $HgCl_2$ were prepared by dissolving $CdCl_2$ or $HgCl_2$ powder (0.2283 and 0.2715 g, respectively) in 10 mL of bi-distilled sterile water under stirring for 10 min to obtain a concentration of 1×10^{-1} M. The $CdCl_2$ or $HgCl_2$ solutions at concentrations of 1×10^{-2}; 1×10^{-3}; 1×10^{-4}; 2×10^{-5}; 1×10^{-6} M were obtained from stock solution by scalar dilution. The solutions of the two different salts were stored at 4 °C until use.

2.3. Cell cultures

Human SH-SY5Y neuroblastoma cells were used in this study. The cells were normally cultured in 25 cm^2 flasks (Corning Inc., NY, USA) and maintained in high glucose (4.5 gL^{-1}) Dulbecco's modified Eagle medium (DMEM), supplemented with 10% (*v*/v) fetal bovine serum (FBS, PAN Biotech), 4 mM L-glutamine (SIGMA), and 1% (v/v) antibiotic solution penicillin-streptomycin (LONZA Bioscience). The cells were maintained at 37 °C in an incubator (Thermo Scientific Hera Cell 240i) with 5% CO_2 in air atmosphere and 95% relative humidity. After being 80% confluent, the cells were washed with phosphate-buffered saline solution (PBS) to remove any unattached cells. The attached cells were harvested using a 1 mL 0.25% trypsin and 0.53 mM EDTA solution (SIGMA) and then seeded at a density of 5×10^3 cells/well in a 96-well plate and incubated for 24 h to allow attachment. In order to monitor the toxicity of Aβ42, Cd^{2+} or Hg^{2+} on SH-SY5Y neuroblastoma cells, we prepared the following experimental sets:

- in the first experimental set, cells were exposed to increasing concentrations of two heavy metals (0.25, 2.5, 25 and 250 μM $CdCl_2$ or $HgCl_2$, 6 wells per concentration group and incubated for 6, 24 and 48 h. Heavy metal was added to the culture media singularly.
- in the second experimental set, cells were exposed to an Aβ42 concentration of 2.5 μM and incubated for 24 h.
- in the third experimental set, cells were exposed to the metal ion-peptide mixtures whose concentrations were 2.5 μM of Aβ42 peptide and scalar concentrations (0.25–250 μM) of Cd^{2+} or Hg^{2+} and incubated for 24 h.
- in the fourth experimental set, cells were left untreated, this being the control group. The control group consists of cells in media (minus the chemical), which are processed identically and incubated simultaneously to the treated groups.

After various time intervals (6, 24 and 48 h), the medium was removed and replaced with 20 μL of MTT stock solution (2 mg/mL in PBS) in 180 μL of medium. Following an additional 3 h of incubation at 37 °C, the medium was removed and 150 μL of DMSO was added to dissolve the formazan crystals, achieved by agitating for 5 min at room temperature. Finally, the absorbance was measured at 540 nm using a multilabel microplate reader Victor 3 (PerkinElmer). All MTT assays were performed in triplicate. Cell viability is defined as the relative absorbance of treated vs. untreated (control), expressed as a percentage.

Results are expressed as mean percentages ± standard error and were evaluated by analysis of variance (ANOVA).

2.4. Single-channel measurement

Channel activity was recorded in PLMs made up of POPC:Chol (70:30, *w*/w) (SIGMA) in 1% n-decane (FLUKA), prepared as previously described [50].

Bilayers were formed across a 300 μm hole in a Teflon partition separating two Teflon chambers (volume 4000 μL) which held symmetrical 0.1 M KCl solutions, pH = 7, temperature 23 ± 1 °C. The aqueous solutions were used unbuffered. The salts used in the experiments were of analytical grade. The Müller-Rudin or painted technique [51–53] was used to form PLMs with lipids solubilised in n-decane. In all Aβ42 experiments performed, the conductance and capacitance of each membrane was tested by applying a voltage of ± 100 mV for 15–20 min under stirring to ensure that the membrane was stable.

To monitor the effect of Cd^{2+} or Hg^{2+} on the peptide in solution, we prepared the following experimental sets:

- in the first experimental set, 6.06 μL of Aβ42 (4.6×10^{-5} M) was diluted in 13.94 μL of $CdCl_2$ or $HgCl_2$ (1×10^{-4} M);
- in the second experimental set, 6.06 μL of Aβ42 (4.6×10^{-5} M) was diluted in 13.94 μL of $CdCl_2$ or $HgCl_2$ (1×10^{-3} M);
- in the third experimental set, 6.06 μL of Aβ42 (4.6×10^{-5} M) was diluted in 13.94 μL of $CdCl_2$ or $HgCl_2$ (1×10^{-2} M);
- in the fourth experimental set, 6.06 μL of Aβ42 (4.6×10^{-5} M) was diluted in 13.94 μL of $CdCl_2$ or $HgCl_2$ (1×10^{-1} M).

After preparation, each metal ion-peptide mixture was stirred for 2 min. For each experimental set, Aβ42 was pre-incubated with metal ions for incubation times of 1 and 24 h at room temperature. Once the bilayer was formed, 14.35 μL of each mixture, carefully stirred for 2 min, was added to the *cis* side of the membrane to obtain the final Aβ42 concentration of 5×10^{-8} M and for each experimental set the following metal ion concentrations:

- in the first experimental set, 0.25 μM of $CdCl_2$ or $HgCl_2$;
- in the second experimental set, 2.5 μM of $CdCl_2$ or $HgCl_2$;
- in the third experimental set, 25 μM of $CdCl_2$ or $HgCl_2$;
- in the fourth experimental set, 250 μM of $CdCl_2$ or $HgCl_2$.

In the single-channel experiments, the membrane current was monitored using the experimental set-up described by Gallucci et al. [54] and Stipani et al. [55] and recorded on a chart recorder for further analysis by hand.

Membrane capacitance was calculated using a calibration curve as described by Micelli et al. [56]. The single-channel data, filtered at 300 Hz as reported by other authors [57] were obtained from at least four experiments performed on different days.

The biophysical and statistical parameters considered to evaluate Aβ42 incorporation pre-incubated with different concentrations of metal ions were single-channel conductance and frequency. To determine conductance, a histogram of the conductance amplitude distribution for each experimental set was constructed and fitted by a Gaussian distribution function. Results are expressed as central conductance ± standard error (Λ_c ± SE) and were evaluated by analysis of variance (ANOVA-Tukey test).

To determine the frequency (number of channels in 60 s), any detection of channel events was counted as successful. Results are expressed as frequency ± standard deviation (F ± SD).

2.5. Electrophoresis and Western blotting

To evaluate the effect of Cd^{2+} or Hg^{2+} on the aggregation state of Aβ42, the peptide was incubated alone or with 0.25, 2.5, 25 μM $CdCl_2$ or $HgCl_2$ at 23 °C for 48 h (T48), 24 h (T24) and 5 min (T0).

Unheated samples in Laemmli sample buffer 1× without SDS were loaded (Aβ42 25 μM per lane) on 4–20% polyacrylamide gel (TGX precast gel, Biorad) without SDS using TGS 1× as running buffer with SDS (0.1%). Electrophoresis was performed for 55 min at 130 V. After electrophoresis, the gel was silver stained.

In addition, Aβ42 was detected by Western blotting, which proved more sensitive for the detection of higher-molecular-mass complexes. Aliquots of different samples were separated by non-denaturing gel electrophoresis and then electrophoretically transferred from gel onto

polyvinylidene difluoride (PVDF) membrane at a constant current of 25 V for 7 min by means of the Trans-Blot® Turbo™ Blotting System (Biorad). The membrane was then blocked with 5% nonfat dry milk-grade blocker (Biorad) in TBS-Tween 0.05% buffer, with gentle agitation for 1 h at room temperature. The blocking solution was replaced with OC antibody produced in rabbit (1:1000 dilution in 5% milk dissolved in TBS-Tween 0.01% buffer) under gentle agitation overnight at 4 °C and subsequently with the secondary polyclonal anti-rabbit IgG antibody conjugated to peroxidase (1:3000 dilution in 5% milk dissolved in TBS-Tween 0.01% buffer) with gentle agitation for 1 h. The blot was developed using the ECL detection system. The blot image was acquired through the ChemiDoc system (Biorad).

2.6. Statistical analysis

The Gaussian distribution function, ANOVA test, Student *t*-test and the fitting procedures were performed using the GraphPad Prism 3 software (GraphPad Prism™ version 3.0). A value of $P < 0.05$ was considered significant.

3. Results

3.1. Cell cultures

Cell viability was measured by the MTT method. This assay is based on the ability of living cells to convert dissolved MTT into insoluble formazan by mitochondrial dehydrogenases. The amount of formazan produced is proportional to the number of living cells [58]. To evaluate the effects of Cd and Hg individually on SH-SY5Y cell viability, we performed cytotoxicity experiments treating the cells with increasing concentrations of both metal ions for different times of incubation. The results of the MTT show that the cytotoxic effect induced by two heavy metals in neuroblastoma cells are dependent on metal concentration and exposure time (Table 1). After 6 h of exposure, the cytotoxic effect of both metals manifests at the concentration of 250 μM and is more evident for Hg^{2+}. At concentrations below 250 μM, the two metal ions do not significantly differ in terms of cell viability compared with the control.

Cells exposed to Cd^{2+} from 0.25 to 250 μM exhibited decreasing percentages of cell viability with increasing metal concentration, showing significant differences in cell viability compared with the control at a 250 μM Cd^{2+} concentration, after 24 h exposure. This cytotoxicity behavior of Cd^{2+} is more evident after 48 h' exposure.

The cytotoxicity of Hg is drastically enhanced at 250 μM, remaining lower and nearly constant at concentrations ranging from 0.25–25 μM after 24 h of exposure. After 48 h exposure, cell death is statistically significant at concentrations of 25 and 250 μM.

The results obtained from the first experimental set seem to indicate that an exposure time of 24 h is sufficient to appreciate the toxic effect of the two metal ions that does not manifest at lower exposure times (6 h, except at the 250 μM concentration) and drastically manifests at the higher exposure time (48 h).

To evaluate the effect of Aβ42 alone on SH-SY5Y cell viability, we performed cytotoxicity experiments treating the cells with peptide alone at a concentration of 2.5 μM for 24 h' incubation (Table 2). The results show that the viability of cells is significantly reduced by 35%.

In light of these considerations, the viability of neuroblastoma cells treated with metal ion-Aβ42 mixtures (third experimental set, see Materials and Methods) was evaluated for an exposure time of 24 h. Table 2 reports the results obtained in these experimental conditions. Both metal ions significantly increase cytotoxicity in a concentration-dependent manner compared to that obtained when treating the cells with Aβ42 peptide or metal ions alone (Table 1, exposure time of 24 h). This result seems to indicate a synergistic toxic effect of Aβ42 and metal ions.

3.2. Single-channel measurement

For all single-channel experiments, PLM stability was tested by performing control experiments with the lipid mixture alone.

The method we used to test PLM stability, either alone or in the presence of Cd and Hg, and to monitor Aβ42 channel activity is as reported in our previous studies [59,60]. Briefly, we carried out: -control experiments to test PLM stability with the lipid mixture alone. The results of these experiments show that the PLMs were stable for long periods of time, with capacitance and conductance values similar to those found in our previous studies (0.30 μF/cm^2 and 13 pS); − experiments in which the peptide was added at the final concentration of 5×10^{-8} M. The characteristics of the channel activity and the lag time (4–5 h) are similar to those reported in our previous studies. Fig. 1 shows an example of chart recordings of Aβ42 channel activity incorporated into POPC:Ch PLMs at the applied voltage of ± 100 mV. The biophysical and statistical values obtained in this work are summarized in Table 3. It is important to note that:

- the central conductance values are dependent on applied voltages, decreasing as the applied voltages increase;
- the central conductance values are symmetrical at positive and negative applied voltages;
- the distribution of the open times follows a one-exponential function, except at an applied voltage of 100 mV;
- the frequency values are independent of applied voltages and are indicative of channel turnover in the membrane.

The pattern obtained in this study is similar to that found in previous studies [59,60].

3.2.1. Aβ42 channel activity pre-incubated for 1 h with Cd^{2+} and Hg^{2+}

Depending on individual propensity and exposure time, several studies highlight the toxic effects of cadmium and mercury in the concentration range of 50–500 μM (47)and > 35- > 200 μg/L [48], respectively. To evaluate the effect of both metal ions on the capacity of

Table 1
Cytotoxic effect of different $CdCl_2$ and $HgCl_2$ concentrations on Cell viability.

Metals	Incubation time (h)	Cell viability (% of control)	Cell viability (% of control)	Cell viability (% of control)	Cell viability (% of control))
		[M] = *0.25 μM*	[M] = *2.5 μM*	[M] = *25* μ*M*	[M] = *250* μ*M*
$CdCl_2$	6	97.82 ± 4.03	97.98 ± 7.02	94.56 ± 6.44	57.80 ± 10.42
$HgCl_2$		98.62 ± 9.43	86.21 ± 2.76	81.97 ± 4.07	32.49 ± 1.44
$CdCl_2$	24	69.87 ± 9.99	66.49 ± 6.11	54.41 ± 4.10	28.97 ± 3.73
$HgCl_2$		79.47 ± 11.45	85.53 ± 18.60	78.19 ± 11.52	28.91 ± 3.97
$CdCl_2$	48	56.34 ± 3.73	36.05 ± 4.70	18.37 ± 3.31	16.46 ± 2.74
$HgCl_2$		86.40 ± 3.26	81.28 ± 9.32	61.11 ± 3.18	16.30 ± 2.46

SH-SY5Y neuroblastoma cells were treated with the indicated concentrations of $CdCl_2$ or $HgCl_2$ for 6, 24 and 48 h. Cell viability was evaluated by the MTT method. The data represented are means ± SE of at least 3 independent experiments.

Table 2
Cytotoxic effect of Aβ42 and Aβ42-metal mixture on Cell viability.

Metals	Cell viability (% of control)	Cell viability (% of control)	Cell viability (% of control)	Cell viability (% of control)	Cell viability (% of control)
	[Aβ42] = *2.5 μM*	[Aβ42 + M] = [*2.5 + 0.25*]*μM*	[Aβ42 + M] = [*2.5 + 2.5*]*μM*	[Aβ42 + M] = [*2.5 + 25*]*μM*	[Aβ42 + M] = [*2.5 + 250*]*μM*
	64.80 ± 6.30	–	–	–	–
$CdCl_2$	-	46.91 ± 3.04	29.81 ± 2.17	20.02 ± 1.99	15.78 ± 1.06
$HgCl_2$	–	55.21 ± 2.19	46.72 ± 7.23	33.36 ± 5.03	16.83 ± 2.45

SH-SY5Y neuroblastoma cells were incubated with Aβ42 and Aβ42-$CdCl_2$ or Aβ42-$HgCl_2$ mixture, at indicated concentrations, for 24 h. Cell viability was evaluated by the MTT method. The data represented are means ± SE of at least 3 independent experiments.

Aβ42 to incorporate into PLMs made up of POPC:Ch (70:30, *w*/w) and to form ion channels, two different sets of experiments were carried out, in which different concentrations of metal ions (0.25, 2.5, 25 μM and 250 μM, corresponding to chronic and acute metal exposure, respectively) were pre-incubated with the peptide for around 1 h. In all experiments, before adding the mixture to the *cis* side of the membrane at an applied voltage of 100 mV (addition voltage), the PLMs were stabilized by applying voltages of ± 100 mV for 15–20 min and monitoring constant values for PLM conductance and capacitance (13 pS and 0.30 μF/cm^2): there was no channel activity in any of these cases. The channel conductance was monitored at applied voltages of ± 80 mV and ± 100 mV; each applied voltage was applied for 60-90 min, starting from 100 mV (i.e. 60-90 min at 100 mV, followed by 60-90 min at −100 mV and so on). Fig. 2 shows examples of chart recordings of Aβ42 channel activity pre-incubated with different $CdCl_2$ or $HgCl_2$ concentrations for 1 h at an applied voltage of 100 mV. Central conductance (Λc ± SE) and frequency (F ± SD) values for the different experimental conditions are reported in Tables 4 and 5, respectively.

It is worth noting that, in the Cd^{2+} 0.25–25 μM concentration range, Aβ42 channel activity begins at the applied voltage of 100 mV (addition and activation voltage) after a lag time that is independent of Cd^{2+} concentration (4 h). The channel activity at an applied voltage of 100 mV was monitored for 1 h; after this time, the applied voltage was shifted to −100 mV for 1 h during which the channel activity began. Decreasing the applied voltage to ± 80 mV, each voltage applied for 90 min, did not lead to channel activity, even upon successive application of voltages as high as ± 120 mV, with each voltage being applied for 1 h. At Cd^{2+} 250 μM, no channel activity was registered after the addition of Cd^{2+}-peptide mixture, even upon application of voltages as high as ± 120 mV (each voltage applied for several hours).

Λ_c values (Λ_c ± SE), after 1 h of pre-incubation of Aβ42 with different Cd^{2+} concentrations, were unchanged in the concentration range of 0.25–25 μM Cd^{2+}. At Cd^{2+} 250 μM, no conductance values are reported owing to the absence of channel activity (Table 4). Besides, the Λ_c values of the Aβ42 channel, in these experimental conditions, seem to be no different than those obtained in the presence of Aβ42 alone at applied voltages of ± 100 mV, where it is possible to compare.

The frequency values (F ± SD) of the Aβ42 channels were not significantly different, suggesting that Cd^{2+}, in the concentration range of 0.25–25 μM, does not affect channel turnover (Table 5). It is important to note that the frequency values obtained in this experimental condition (1 h incubation and concentration range of 0.25–25 μM Cd^{2+}) are significantly different than those obtained in the presence of Aβ42 alone, suggesting that Cd^{2+} promotes both the conformational changes and the peptide aggregation that makes the peptide less able to interact with PLMs and form ion channels.

Table 3
Characteristic parameters of Aβ42 channels in POPC:Chol PLMs.

Vs mV	Λc ± SE nS	F ± SD	τ_1 s	τ_2 s
100	0.020 ± 0.0006	10.52 ± 0.13	0.18	0.95
80	0.029 ± 0.002	11.12 ± 0.10	0.87	
−80	0.030 ± 0.0005	10.83 ± 0.15	1.48	
−100	0.021 ± 0.003	10.02 ± 0.18	1.21	

The mean conductance fitted by Gaussian distribution (Λc ± SE), the frequency (F ± SD), the life time (τ) of the Aβ42 channels at different applied voltages in POPC:Chol PLMs. The minimum and maximum number of channels considered (N) out of a total number of channels considered (Nt) was: 1503 < *N* < 8615, Nt = 18653.

The behavior of the Aβ42 channel, pre-incubated for 1 h with different concentrations of Hg^{2+} (0.25, 2.5, 25 and 250 μM), seems to be different than that obtained in the presence of Cd^{2+}. In all experiments, at concentrations of 0.25 and 2.5 μM, channel activity appears at an applied voltage of 100 mV (addition and activation voltage) and goes on showing at applied voltages of −100 and ± 80 mV. At an Hg^{2+} concentration of 25 μM, channel activity was only registered at an applied voltage of ± 100 mV, while at the higher concentration (250 μM) no channel activity was observed even upon application of voltages as high as ± 120 mV (each voltage applied for several hours).

Table 4 reports the central conductance values (Λ_c ± SE) where it can be seen that at an Hg^{2+} concentration of 0.25 μM, Λ_c values are dependent on the applied voltage to the membrane decreasing as the voltage is increased and are not significantly different from those of Aβ42 alone. At an Hg^{2+} concentration of 2.5 μM, conductance values

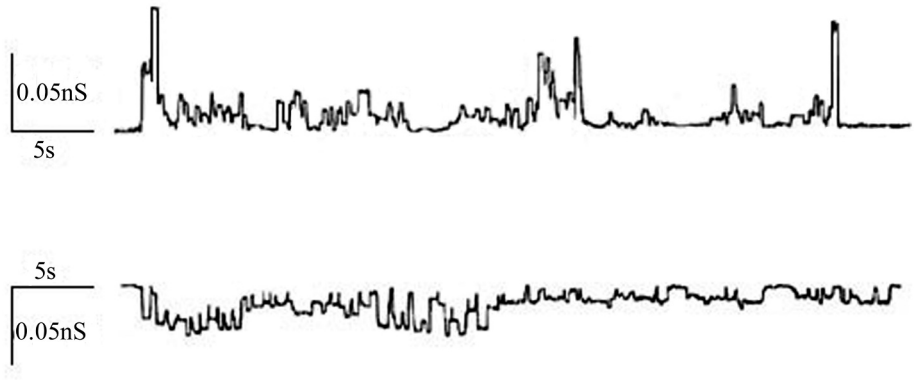

Fig. 1. Aβ42 channel activity in POPC:Ch PLMs. Representative traces illustrating channel activity of Aβ42 in membranes made up of POPC:Ch (70:30,w:w) recorded after an average of one hour from first channel formation, when channel activity is substantial and lasting. Applied voltage was set to 100 mV (top trace) and − 100 mV (bottom trace). Experiments were performed in the presence of Aβ42 (5×10^{-8} M) added to the *cis* side, while the aqueous phase contained 0.1 M KCl (pH 7) and *T* = 23 ± 1 °C.

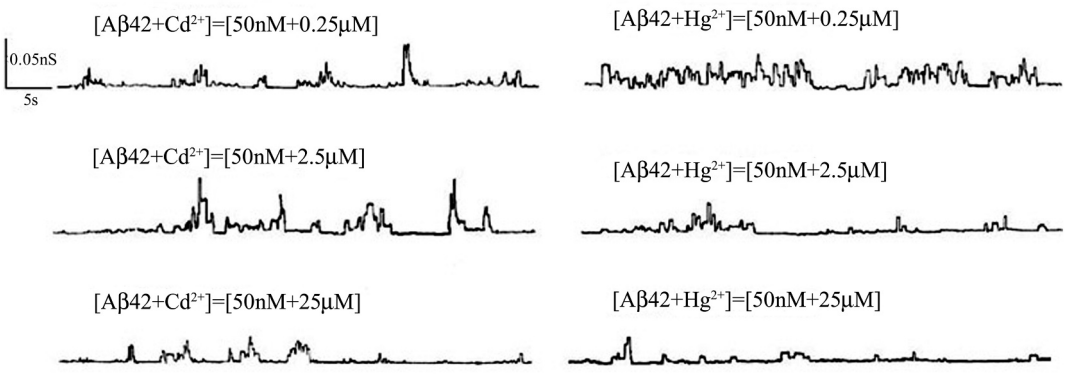

Fig. 2. Aβ42 channel activity preincubated with $CdCl_2$ and $HgCl_2$ for 1 h. Representative traces illustrating channel activity of Aβ42 in membranes made up of POPC:Ch (70:30,w:w) preincubated with different concentrations of $CdCl_2$ and $HgCl_2$ for 1 h. Channel activity was recorded after an average of 30 min from first channel formation, when channel activity is substantial and lasting. Applied voltage was set to 100 mV. Experimental conditions: KCl 0.1 M (pH 7) and T = 23 ± 1 °C.

are independent of applied voltage to the membrane and significantly lower than those for Aβ42 alone.

The frequency values (Table 5) are directly correlated with applied voltage to the membrane at an Hg^{2+} 0.25 μM concentration and significantly lower than those for Aβ42 alone at applied voltages of ± 80 mV. At an Hg^{2+} concentration of 2.5 μM, frequency values are independent of applied voltages and significantly lower than those of Aβ42 alone. The frequency values decrease further at an Hg^{2+} concentration of 25 μM.

The results obtained from experiments before incubation with both metal ions for 1 h seem to indicate that: - Cd^{2+} and Hg^{2+} inhibit Aβ42 incorporation into PLMs due to a decrease in channel turnover; − Cd^{2+}, at concentrations ranging from 0.25–25 μM, and Hg^{2+}, at the 0.25 μM concentration, do not affect the conductance values of the Aβ42 channel more than those obtained in presence of Aβ42 alone; − Hg^{2+}, at the concentrations of 2.5 and 25 μM, decreases the conductance of the Aβ42 channel suggesting that this metal ion favours the formation of aggregates that assemble into PLMs to form conductive pathways smaller than those in the presence of Aβ42 alone.

3.2.2. *Aβ42 channel activity pre-incubated for 24 h with Cd^{2+} and Hg^{2+}*

To evaluate the inhibitory effect of Cd^{2+} and Hg^{2+} on Aβ42 incorporation into PLMs and its channel activity after incubation for longer than 1 h, we carried out two sets of experiments in which the scalar concentrations of both metal ions (0.25, 2.5, 25 and 250 μM) were pre-incubated with the peptide around 24 h. Using the same protocol described for the first experimental sets, we monitored Aβ42 incorporation and channel activity at applied voltages of ± 100 mV and ± 80 mV. Fig. 3 shows examples of chart recordings of Aβ42 channel activity pre-incubated with different $CdCl_2$ or $HgCl_2$ concentrations for 24 h at an applied voltage of 100 mV. The central conductance (Λ_c ± SE) and frequency (F ± SD) values are reported in Tables 6 and 7, respectively.

At Cd^{2+} concentrations of 0.25 and 2.5 μM, Aβ42 channel activity manifests at applied voltages of ± 100 mV, characterized by frequency values that decrease as the metal ion concentration increases. Where it is possible to compare, central conductance values are fundamentally lower than those obtained with Aβ42 alone. At applied voltages of ± 80 mV, each voltage applied for 90 min, no channel activity was observed even upon successive application of voltages as high as ± 120 mV (each voltage applied for 1 h). At higher Cd^{2+} concentrations (25 and 250 μM), no channel activity was recorded, even upon application of voltages as high as ± 120 mV for several hours.

In pre-incubation experiments with Hg^{2+}, Aβ42 channel activity appears in the concentration range of 0.25–2.5 μM, characterized by frequency values inversely correlated with metal ion concentration, decreasing as the latter concentration increases (Table 7). At an Hg^{2+} concentration of 0.25 μM and at applied voltages of 80 and − 100 mV, central conductance values are lower than those obtained with Aβ42 alone, while at concentrations of 2.5 and 25 μM conductance values are significantly lower than those of Aβ42 alone at applied voltages where it is possible to compare. At 250 μM, no channel activity was found, even upon application of voltages as high as ± 120 mV for several hours.

The results obtained from these experimental sets indicate that the inhibitory effect of both ion metals on Aβ42 incorporation and channel turnover is more evident after 24 h of pre-incubation, than after 1 h, decreasing until channel activity disappears. This effect could depend on the ability of Cd^{2+} and Hg^{2+} to favour the formation of Aβ42 aggregates that are unable to interact with the membrane.

3.3. *Electrophoresis and Western blot*

We evaluated the aggregation state of the Aβ42 peptide in the absence and presence of Cd^{2+} or Hg^{2+} by electrophoresis and Western blotting. Analysis of Aβ42 by non-denaturing PAGE in the sample at time zero showed monomers, trimers, tetramers and pentamers with an apparent molecular weight (MW) of 4.5, 13.5, 18 and 22.5 kDa, respectively. After 24 and 48 h of incubation, an increase in 13.5 and 22.5 kDa species was observed, and a band with an apparent MW of 27 kDa was more evident than at time zero (Fig. 4). After electrophoresis, the samples were blotted onto a PVDF membrane, which was stained for Aβ42 immunoreactivity. Western blot analysis of Aβ42 samples with OC antibody showed peptide immunoreactive bands with apparent molecular masses of 4.5, 13.5, 18 and 22.5 kDa (Fig. 4). A band with an apparent MW of 27 kDa and larger aggregates ranging from 50 to 75 kDa were detected after 24 h' incubation and even more so after 48 h. Additionally, the trimer and pentamer bands were more marked as incubation time increased. Fig. 4 shows that aggregate species remained inside the wells.

Electrophoretic analysis of the Aβ42 peptide incubated with different Cd^{2+} concentrations (0.25, 2.5 and 25 μM) showed monomers, trimers, tetramers, pentamers and hexamers. The band with an apparent MW of 27 kDa seems to be quite faint. Western blot analysis of samples incubated with Cd^{2+} confirmed the results obtained with electrophoresis. Additionally, larger aggregates ranging from 37 to 150 kDa were detected after incubation for 48 and 24 h for all Cd^{2+} concentrations (Fig. 5). It is important to note that the signal intensity of larger aggregates is more evident after 24 h of incubation when Cd^{2+} concentration is 2.5 μM than that detected at 0.25 and 25 μM at the

Table 4
Mean conductance of Aβ42 channel pre-incubated with different $CdCl_2$ and $HgCl_2$ concentrations for 1 h.

Vs mV	[Aβ + Cd^{2+}] [5 × 10^{-8} M + 0.25 μM	[Aβ + Cd^{2+}] [5 × 10^{-8} M + 2.5 μM	[Aβ + Cd^{2+}] [5 × 10^{-8} M + 25 μM	[Aβ + Cd^{2+}] [5 × 10^{-8} M + 250 μM	[Aβ + Hg^{2+}] [5 × 10^{-8} M + 0.25 μM	[Aβ + Hg^{2+}] [5 × 10^{-8} M + 2.5 μM	[Aβ + Hg^{2+}] [5 × 10^{-8} M + 25 μM	[Aβ + Hg^{2+}] [5 × 10^{-8} M + 250 μM
	Λc ± SE nS	Λc ± SE nS	Λc ± SE nS	Λc ± SE nS	Λc ± SE nS	Λc ± SE nS	Λc ± SE nS	Λc ± SE nS
100	0.020 ± 0.001	0.020 ± 0.001	0.016 ± 0.002	–	0.018 ± 0.0005	0.012 ± 0.0050	0.010 ± 0.0008	–
80	–	–	–	–	0.025 ± 0.0020	0.011 ± 0.0020	–	–
−80	–	–	–	–	0.029 ± 0.0020	0.012 ± 0.001	–	–
−100	0.021 ± 0.002	0.019 ± 0.002	0.015 ± 0.005	–	0.020 ± 0.0010	0.014 ± 0.0080	0.011 ± 0.0009	–

The central conductance ± standard error (Λ_c ± SE) of the Aβ42 channel pre-incubated with 0.25, 2.5, 25 and 250 μM of $CdCl_2$ and $HgCl_2$ in POPC:Ch PLMs. The minimum and maximum number of channels considered (N) out of a total number of channels considered (N_t) was: [Aβ42] + [Cd^{2+}] = 5 × 10^{-8} M + 0.25 μM, 350 < N < 609, Nt = 959; [Aβ42] + [Cd^{2+}] = 5 × 10^{-8} M + 2.5 μM, 216 < N < 252, Nt = 468; [Aβ42] + [Cd^{2+}] = 5 × 10^{-8} M + 25 μM, 106 < N < 114, Nt = 220; [Aβ42] + [Hg^{2+}] = 5 × 10^{-8} M + 0.25 μM, 358 < N < 2375, Nt = 4626; [Aβ42] + [Hg^{2+}] = 5 × 10^{-8} M + 2.5 μM, 102 < N < 198, Nt = 486; [Aβ42] + [Hg^{2+}] = 5 × 10^{-8} M + 25 μM, 101 < N < 112, Nt = 213.

Table 5
Channel frequency of Aβ42 pre-incubated with different $CdCl_2$ and $HgCl_2$ concentrations for 1 h.

Vs mV	[Aβ + Cd^{2+}] [5 × 10^{-8} M + 0.25 μM	[Aβ + Cd^{2+}] [5 × 10^{-8} M + 2.5 μM	[Aβ + Cd^{2+}] [5 × 10^{-8} M + 25 μM	[Aβ + Cd^{2+}] [5 × 10^{-8} M + 250 μM	[Aβ + Hg^{2+}] [5 × 10^{-8} M + 0.25 μM	[Aβ + Hg^{2+}] [5 × 10^{-8} M + 2.5 μM	[Aβ + Hg^{2+}] [5 × 10^{-8} M + 25 μM	[Aβ + Hg^{2+}] [5 × 10^{-8} M + 250 μM
	F ± SD	F ± SD	F ± SD	F ± SD	F ± SD	F ± SD	F ± SD	F ± SD
100	3.07 ± 0.46	3.05 ± 0.28	4.47 ± 0.44	–	7.64 ± 0.36	1.36 ± 0.31	0.55 ± 0.10	–
80	–	–	–	–	2.74 ± 0.15	2.17 ± 0.34	–	–
−80	–	–	–	–	1.10 ± 0.12	0.81 ± 0.19	–	–
−100	4.73 ± 0.28	5.09 ± 0.48	4.21 ± 0.43	–	9.08 ± 0.81	1.48 ± 0.17	0.49 ± 0.08	–

The frequency ± standard deviation (F ± SD) of the Aβ42 channel pre-incubated with 0.25, 2.5, 25 and 250 μM of $CdCl_2$ and $HgCl_2$ in POPC:Ch PLMs. The minimum and maximum number of channels considered (N) out of a total number of channels considered (N_t) is reported in the legend to Table 2.

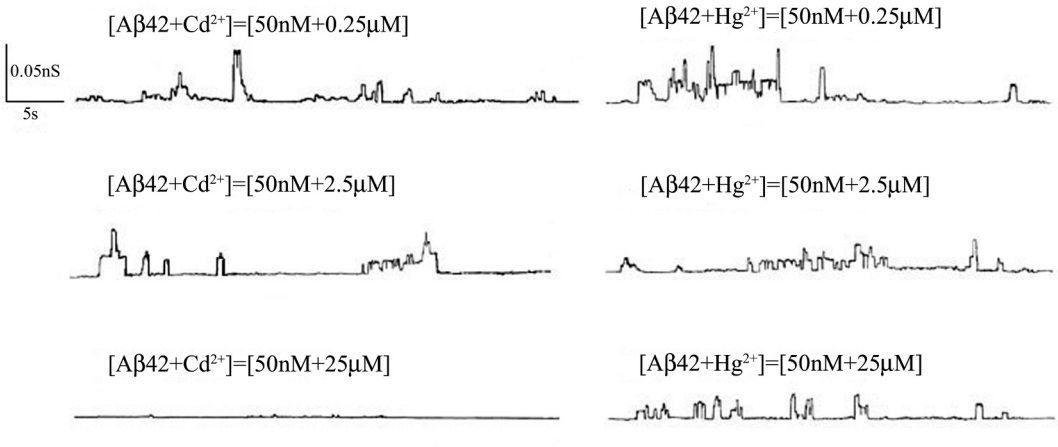

Fig. 3. Aβ42 channel activity preincubated with $CdCl_2$ and $HgCl_2$ for 24 h. Representative traces illustrating channel activity of Aβ42 in membranes made up of POPC:Ch (70:30,w:w) preincubated with different concentrations of $CdCl_2$ and $HgCl_2$ for 24 h. Channel activity was recorded after an average of 30 min from first channel formation, when channel activity is substantial and lasting. Applied voltage was set to 100 mV. Experimental conditions: KCl 0.1 M (pH 7) and T = 23 ± 1 °C.

same incubation time. This result is in line with that obtained in our previous study using Circular Dichroism (CD) indicating that sub-stoichiometric amounts of Cd^{2+} can induce secondary structure transition of Aβ42 compatible with amyloid aggregates [59].

The results of electrophoretic analysis of Aβ42 peptide incubated with Hg^{2+} ranging from 0.25 to 25 μM are similar to those obtained with Cd^{2+}, showing bands with an apparent MW of 4.5, 13.5, 18, 22.5 and 27 kDa (Fig. 6). The intensity of the 27 kDa band decreases in a more evident manner over the course of time, starting from time 0 up to 48 h, when the Hg^{2+} concentration is 25 μM than other concentrations. Western blot analysis of the Aβ42 samples with Hg^{2+} showed bands of monomers, trimers and pentamers whose intensities increase over time, starting from time 0 up to 48 h. In the Aβ42 samples with 0.25 μM Hg^{2+}, a band of hexamers can be seen, whose intensity decreases with increase of the incubation time and larger aggregates ranging from 37 to 150 kDa at 48 h incubation time. In the Aβ42 samples with 2.5 and 25 μM Hg^{2+}, the larger aggregates were detected after 24 h (Fig. 6). To better appreciate the effect of Cd^{2+} and Hg^{2+} on the Aβ42 aggregation process, Fig. 7 shows a synoptic image in which the immunoreactive bands in the absence and presence of both metal ions are shown after 24 h of incubation. It can be seen that the immunoreactive bands of large aggregates present higher signal intensity and molecular weight range, in the presence of 2.5 μM Cd^{2+} or Hg^{2+} than those in the presence of Aβ42 alone. Besides, the incubation of Aβ42 with the two metal ions increases the signal intensity of the pentamer bands while decreasing that of the trimer bands. These results indicate that the two metal ions favour both the formation of high-molecular-weight aggregates and low-molecular-weight oligomers.

4. Discussion

In the last few years, many researchers have studied AD pathogenesis, and its molecular mechanisms are still the subject of intensive research. An increasing number of studies have highlighted the fact that peptides Aβ42 and Aβ40 present a high propensity to form oligomeric species that have shown to be more toxic than fibrils. The conversion of peptides from a native soluble form to a non-native – often insoluble – form seems to be favoured by metal ions that are able to bind to the Aβ molecules, as in-vitro studies have shown [27,29,30], and are present in senile plaques of AD patients, as post-mortem studies of human brains have revealed [25,61,62]. In addition, Cd^{2+} and Hg^{2+}, known environmental contaminants, affect different organs and organ systems, most importantly the central nervous system. Several studies have provided evidence of links between AD and these two heavy metals [44,46,63,64]. For these reasons, we investigated the effect of Cd^{2+} and Hg^{2+} different concentrations on the Aβ42 peptide by various methods.

Our cell-viability experiments show that the toxicity of the Aβ42 peptide is significantly increased when cells are exposed to metal ion-Aβ42 mixtures, suggesting that the toxic effects of Aβ42 are most potent in the presence of heavy metals. Our results seem to be in line with those obtained by other authors, showing that different metal ions modulate Aβ42 toxicity [21,39,41,42]. To explore whether the higher cytotoxicity observed when the cells were treated with a mixture of Aβ42 and metal ions could also be directly due to the effects of metal ions on the Aβ42 molecule, we carried out pre-incubation experiments using a single-channel measurement method. It evaluated the capacity of the Aβ42 peptide, pre-incubated with different concentrations of Cd^{2+} or Hg^{2+}, to incorporate and form ion channels in PLMs made up of POPC:Ch (70:30, *w*/w). In our previous studies we shown that Cd^{2+} and Hg^{2+} are able to interact with the Aβ42 peptide by acting on the channel incorporated into the membrane [59,60], in this study we evaluated the effects of Cd^{2+} and Hg^{2+} on the Aβ42 peptide in solution. The results show that both metal ions, despite their differences in conductance and frequency values, decrease the capacity of the peptide to incorporate and form ion channels until channel activity has been completely eliminated more than the Aβ42 peptide alone. The peptide's lower capacity to form ion channels until its disappearance depend on metal ion concentration and on incubation time. These results suggest that both metal ions can promote changes in the peptide's secondary structure that favour the formation of large aggregates that are not prone to incorporating into PLMs, as demonstrated by circular dichroism (CD) in our previous studies [59,60]. Cd^{2+} and Hg^{2+} are able to bind to the imidazole and carboxyl groups in proteins or peptides, thus promoting the formation of stable polydentate complexes that inhibit protein folding or refolding and favour the aggregation process [65]. The capacity of Cd^{2+} and Hg^{2+} to bind to Aβ42 molecules has been shown in numerous studies [30,59,60,66,67].

The formation of ion channels in PLMs containing cholesterol and the presence of the sterol in biomembranes can be considered protective factors against Aβ-metal complex toxicity [50,59,68,69]. The addition of cholesterol to the membrane made up of POPC shifts the ion selectivity of the Aβ42 channel from cation to neutral, thus shifting the membrane potential away from the threshold of membrane excitability and, therefore, decreasing Ca^{2+} permeability, which is thought to determine degeneration of neurons [70]. Besides, the cholesterol molecule, by favouring Aβ42 insertion into the membrane, shifts the balance toward clearance, a mechanism that removes Aβ42 molecules from the fibrillation process [69]. In the light of our results and those from the

Table 6
Mean conductance of Aβ42 channel pre-incubated with different $CdCl_2$ and $HgCl_2$ concentrations for 24 h.

Vs mV	[Aβ + Cd^{2+}] [5 × 10^{-8} M + 0.25 μM	[Aβ + Cd^{2+}] [5 × 10^{-8} M + 2.5 μM	[Aβ + Cd^{2+}] [5 × 10^{-8} M + 25 μM	[Aβ + Cd^{2+}] [5 × 10^{-8} M + 250 μM	[Aβ + Hg^{2+}] [5 × 10^{-8} M + 0.25 μM	[Aβ + Hg^{2+}] [5 × 10^{-8} M + 2.5 μM	[Aβ + Hg^{2+}] [5 × 10^{-8} M + 25 μM	[Aβ + Hg^{2+}] [5 × 10^{-8} M + 250 μM
	Λc ± SE nS	Λc ± SE nS	Λc ± SE nS	Λc ± SE nS	Λc ± SE nS	Λc ± SE nS	Λc ± SE nS	Λc ± SE nS
100	0.016 ± 0.002	0.013 ± 0.004	–	–	0.020 ± 0.001	0.010 ± 0.008	0.010 ± 0.010	–
80	–	–	–	–	0.023 ± 0.001	0.014 ± 0.006	–	–
−80	–	–	–	–	–	–	–	–
−100	0.017 ± 0.002	0.017 ± 0.0004	–	–	0.015 ± 0.0006	–	0.011 ± 0.009	–

The central conductance ± standard error (Λ_c ± SE) of the Aβ42 channel pre-incubated with 0.25, 2.5, 25 and 250 μM of $CdCl_2$ and $HgCl_2$ in POPC:Ch PLMs. The minimum and maximum number of channels considered (N) out of a total number of channels considered (N_t) was: [Aβ42] + [Cd^{2+}] = 5 × 10^{-8} M + 0.25 μM, 241 < *N* < 306, Nt = 547; [Aβ42] + [Cd^{2+}] = 5 × 10^{-8} M + 2.5 μM, 201 < *N* < 223, Nt = 424; [Aβ42] + [Hg^{2+}] = 5 × 10^{-8} M + 0.25 μM, 367 < *N* < 656, Nt = 1478; [Aβ42] + [Hg^{2+}] = 5 × 10^{-8} M + 2.5 μM, 134 < *N* < 174, Nt = 308; [Aβ42] + [Hg^{2+}] = 5 × 10^{-8} M + 25 μM, 98 < *N* < 108, Nt = 206.

Table 7
Channel frequency of Aβ42 pre-incubated with different $CdCl_2$ and $HgCl_2$ concentrations for 24 h.

Vs mV	[Aβ + Cd^{2+}] [5 × 10^{-8} M + 0.25 μM	[Aβ + Cd^{2+}] [5 × 10^{-8} M + 2.5 μM	[Aβ + Cd^{2+}] [5 × 10^{-8} M + 25 μM	[Aβ + Cd^{2+}] [5 × 10^{-8} M + 250 μM	[Aβ + Hg^{2+}] [5 × 10^{-8} M + 0.25 μM	[Aβ + Hg^{2+}] [5 × 10^{-8} M + 2.5 μM	[Aβ + Hg^{2+}] [5 × 10^{-8} M + 25 μM	[Aβ + Hg^{2+}] [5 × 10^{-8} M + 250 μM
	F ± SD	F ± SD	F ± SD	F ± SD	F ± SD	F ± SD	F ± SD	F ± SD
100	3.22 ± 0.19	1.23 ± 0.08	–	–	2.40 ± 0.47	0.77 ± 0.13	0.65 ± 0.06	–
80	–	–	–	–	3.98 ± 0.79	0.88 ± 0.19	–	–
−80	–	–	–	–	–	–	–	–
−100	4.32 ± 0.28	0.87 ± 0.06	–	–	5.91 ± 0.91	–	0.66 ± 0.07	–

The frequency ± standard deviation (F ± SD) of the Aβ42 channel pre-incubated with 0.25, 2.5, 25 and 250 μM of $CdCl_2$ and $HgCl_2$ in POPC:Ch PLMs. The minimum and maximum number of channels considered (N) out of a total number of channels considered (N_t) is reported in the legend to Table 4.

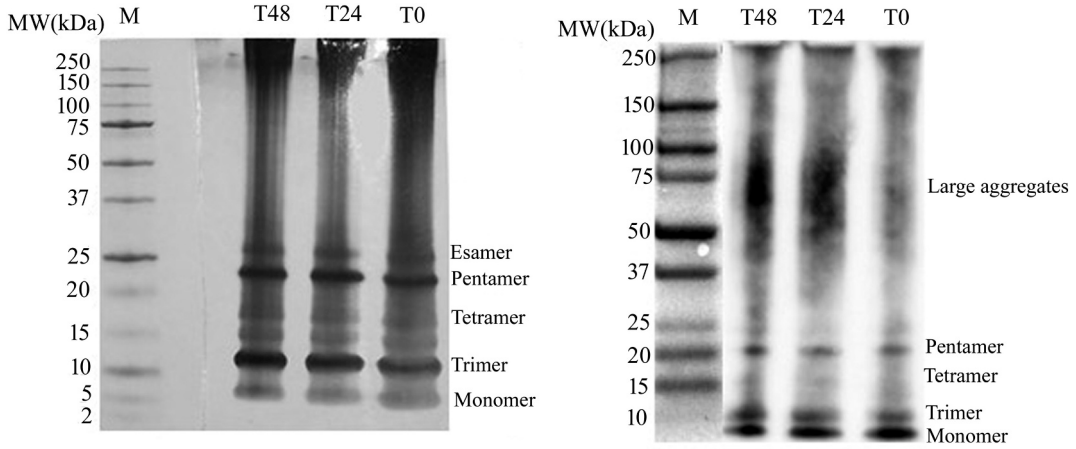

Fig. 4. Aggregation states of Aβ42 peptide analysed with non-denaturing Electrophoresis and Western blot. a Non-denaturing PAGE of Aβ42 samples: MW, molecular weight ladder; M, marker; T0, Aβ42 sample removed from stock solution and analysed; T24 and T48, Aβ42 samples after 24 and 48 h of incubation, respectively. b Western blot analysis of Aβ42 aggregates separated on a 4–20% non-denaturing polyacrylamide gel with the polyclonal conformational antibody OC. Experimental conditions: [Aβ42] = 25 μM; T = 23 ± 1 °C.

literature, we hypothesize that Cd^{2+} or Hg^{2+}, by binding to specific aminoacids, promote the formation of aggregates that are not prone to incorporate into PLMs and to form ion channels.

To verify that the two metal ions favour the formation of high-molecular-weight aggregates, we carried out electrophoresis and western blot experiments on Aβ42 alone and Aβ42 incubated with Cd^{2+} or Hg^{2+}, at the concentrations of 0.25, 2.5 and 25 μM and for different incubation times. The results obtained from these experiments show that the two ions promote the formation of both low molecular weight aggregates (trimers, tetramers, pentamers) and of high-molecular-weight ones after 24–48 h of incubation (large aggregates). The formation of large aggregates seems to depend on metal ion concentration, and – in the case of Cd^{2+}/Hg^{2+} – sub/equi-stoichiometric amounts (2.5/25 μM, respectively) favour the formation of high-molecular-weight aggregates, confirming the results obtained by single-channel measurements. These results are in line with those obtained with CD

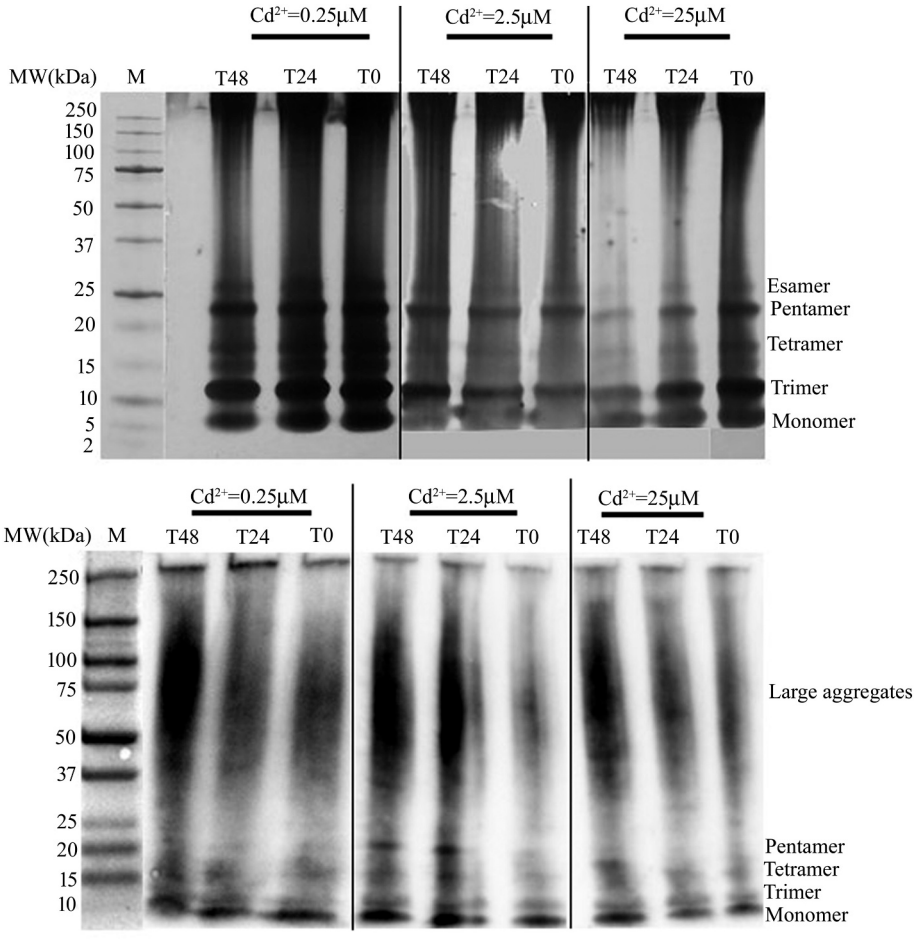

Fig. 5. Aggregation states of Aβ42 peptide in presence of $CdCl_2$ analysed with non-denaturing Electrophoresis and Western blot. a Non-denaturing PAGE of Aβ42 samples incubated with different $CdCl_2$ concentrations: MW, molecular weight ladder; M, marker; T0, Aβ42 + Cd^{2+} sample analysed after the preparation; T24 and T48, Aβ42 + Cd^{2+} samples after 24 and 48 h of incubation, respectively. b Western blot analysis of Aβ42 + Cd^{2+} aggregates separated on a 4–20% non-denaturing polyacrylamide gel with the polyclonal conformational antibody OC.
Each sample contains 25 μM Aβ42 with different Cd^{2+} concentrations: Experimental conditions: T = 23 ± 1 °C.

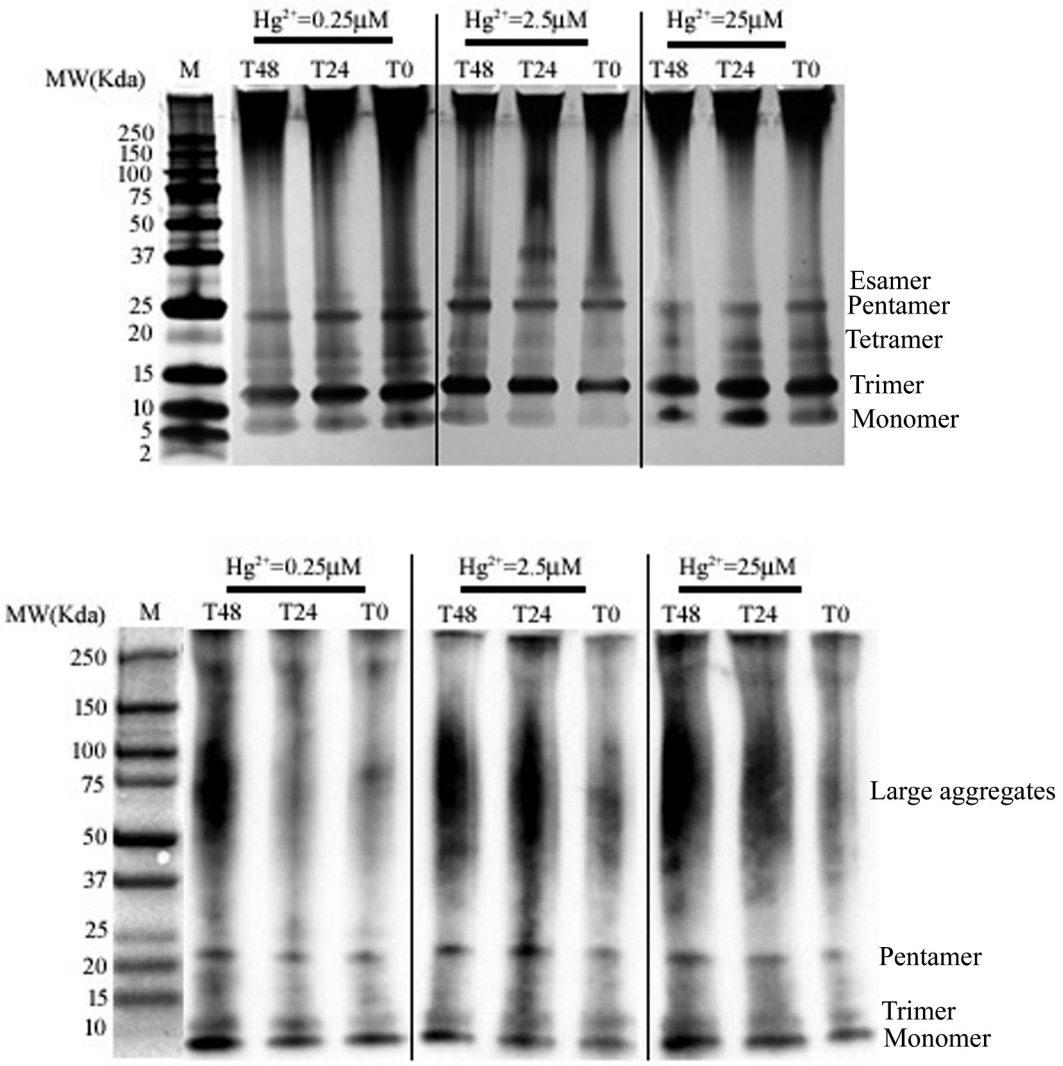

Fig. 6. Aggregation states of Aβ42 peptide in presence of $HgCl_2$ analysed with non-denaturing Electrophoresis and Western blot. a Non-denaturing PAGE of Aβ42 samples incubated with different $HgCl_2$ concentrations: MW, molecular weight ladder; M, marker; T0, Aβ42 + Hg^{2+} sample analysed after the preparation; T24 and T48, Aβ42 + Hg^{2+} samples after 24 and 48 h of incubation, respectively. b Western blot analysis of Aβ42 + Hg^{2+} aggregates separated on a 4–20% non-denaturing polyacrylamide gel with the polyclonal conformational antibody OC.
Each sample contains 25 μM Aβ42 with different Hg^{2+} concentrations: Experimental conditions: T = 23 ± 1 °C.

and reported in our previous study [59,60]. A recent study on the identification of on-and off-pathway oligomers in amyloid fibril formation shows that, for Aβ42 in buffer, its oligomers are found to only form in appreciable amounts in the presence of both monomers and fibrils, suggesting that Aβ42 oligomers dissociate to monomers, but are constantly reformed, thus contributing to the formation of fibrils [71]. Several studies show that Aβ42 interacts with lipid membranes to form an ion channel [69,70,72,73] constituted by between four and six Aβ42 monomers. Tetramers and hexamers seem to be the most stable structures in lipid bilayers, although the formation of larger structures in lipid bilayers cannot be excluded [74]. Similar structures have been observed for other amyloid polypeptides, such as α-synuclein and human amylin (hIAPP). The results obtained by Scalisi and colleagues suggest a possible mechanism for membrane damage by hIAPP due to the formation of cylindrical structures (derived from protofibrils) assembled in membrane pores, and not to the formation of mature fibrils. In the model proposed by Scalisi and colleagues, the off-pathway oligomers are in equilibrium with monomers which immediately enter the membrane [75]. On the other hand, the extracellular accumulation of 56KDa soluble oligomers (dodecamers) in Tg2576 mice produces memory deficits, indicating that monomers or fibrils are less toxic than soluble oligomers [76]. If the results obtained by the above authors are combined with ours, it is plausible to speculate that Aβ42 toxicity is increased by Cd^{2+} or Hg^{2+}, by promoting the formation of both low-molecular-weight oligomers that, by incorporating into the membrane, can form pores and high-molecular-weight aggregates that, by accumulating outside the cell membrane or constituting a reservoir of monomers, can produce cell damage.

The results presented in this study show that Cd^{2+} and Hg^{2+} affect the Aβ42 peptide, increasing its cytotoxicity and favouring the formation of different-sized aggregates (low- and high-molecular-weight oligomers) and strengthening the hypothesis that the two metals, known environmental pollutants, may be cofactors of risk for AD.

Author statement

The authors have nothing to declare.

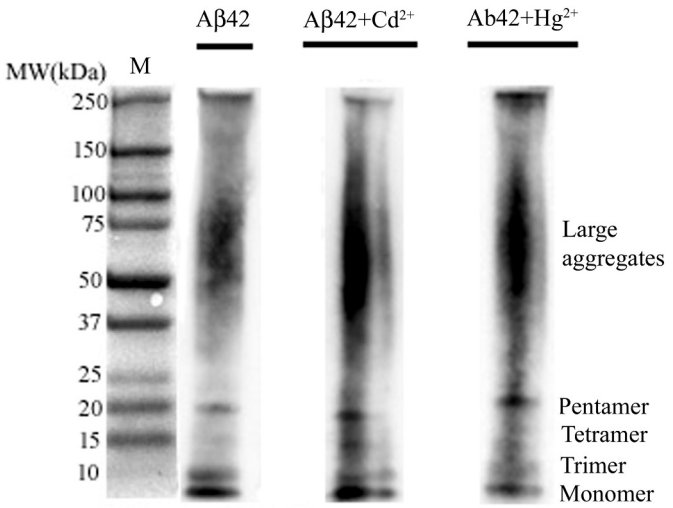

Fig. 7. Aggregation states of Aβ42 peptide in the absence and presence of $CdCl_2$ and $HgCl_2$ analysed with Western blot. The synoptic image reports the Western blot analysis of Aβ42 alone and Aβ42 incubated with 2.5 μM of Cd^{2+} or Hg^{2+} for 24 h. MW, molecular weight ladder; M, marker. Experimental conditions: [Aβ42] = 25 μM; T = 23 ± 1 °C.

Declaration of Competing Interest

The authors declare that the research was conducted in the absence of any commercial or financial relationships that could be construed as a potential conflict of interest.

Acknowledgments

The authors acknowledge Anthony Green for proofreading and providing linguistic advice.

References

[1] R. Katzman, R. Terry, R. DeTeresa, T. Brown, P. Davies, P. Fuld, et al., Clinical, pathological, and neurochemical changes in dementia: a subgroup with preserved mental status and numerous neocortical plaques, Ann. Neurol. 23 (2) (1988) 138–144.
[2] J.L. Price, J.C. Morris, Tangles and plaques in nondemented aging and "preclinical" Alzheimer's disease, Ann. Neurol. 45 (3) (1999) 358–368.
[3] H.J. Aizenstein, R.D. Nebes, J.A. Saxton, J.C. Price, C.A. Mathis, N.D. Tsopelas, et al., Frequent amyloid deposition without significant cognitive impairment among the elderly, Arch. Neurol. 65 (11) (2008) 1509–1517.
[4] O. Zolochevska, G. Taglialatela, Non-demented individuals with Alzheimer's disease neuropathology: resistance to cognitive decline may reveal new treatment strategies, Curr. Pharm. Des. 22 (26) (2016) 4063–4068.
[5] B. Caughey, P.T. Lansbury, Protofibrils, pores, fibrils, and neurodegeneration: separating the responsible protein aggregates from the innocent bystanders, Annu. Rev. Neurosci. 26 (2003) 267–298.
[6] C.G. Glabe, Common mechanisms of amyloid oligomer pathogenesis in degenerative disease, Neurobiol. Aging 27 (4) (2006) 570–575.
[7] S. Lesné, L. Kotilinek, K.H. Ashe, Plaque-bearing mice with reduced levels of oligomeric amyloid-beta assemblies have intact memory function, Neuroscience. 151 (3) (2008) 745–749.
[8] L. Lue, Y. Kuo, A. Roher, L. Brachova, Y. Shen, L. Sue, et al., Soluble amyloid beta peptide concentration as a predictor of synaptic change in Alzheimer's disease, Am. J. Pathol. 155 (3) (1999) 853–862.
[9] C. McLean, R. Cherny, F. Fraser, S. Fuller, M. Smith, K. Beyreuther, et al., Soluble pool of Abeta amyloid as a determinant of severity of neurodegeneration in Alzheimer's disease, Ann. Neurol. 46 (6) (1999) 860–866.
[10] R. Roychaudhuri, M. Yang, M.M. Hoshi, D.B. Teplow, Amyloid beta-protein assembly and Alzheimer disease, J. Biol. Chem. 284 (8) (2009) 4749–4753.
[11] J. Tsai, J. Grutzendler, K. Duff, W.B. Gan, Fibrillar amyloid deposition leads to local synaptic abnormalities and breakage of neuronal branches, Nat. Neurosci. 7 (11) (2004) 1181–1183.
[12] K. Matsuzaki, T. Noguch, M. Wakabayashi, K. Ikeda, T. Okada, Y. Ohashi, et al., Inhibitors of amyloid beta-protein aggregation mediated by GM1-containing raft-like membranes, Biochim. Biophys. Acta 1768 (1) (2007) 122–130.
[13] V. Saranya, P.V. Mary, S. Vijayakumar, R. Shankar, The hazardous effects of the environmental toxic gases on amyloid beta-peptide aggregation: a theoretical perspective, Biophys. Chem. 263 (2020) 106394.
[14] M.C. Owen, D. Gnutt, M. Gao, S.K.T.S. Wärmländer, J. Jarvet, A. Gräslund, et al., Effects of in vivo conditions on amyloid aggregation, Chem. Soc. Rev. 48 (14) (2019) 3946–3996.
[15] K. Matsuzaki, K. Kato, K. Yanagisawa, Abeta polymerization through interaction with membrane gangliosides, Biochim. Biophys. Acta 1801 (8) (2010) 868–877.
[16] S.A. Kotler, P. Walsh, J.R. Brender, A. Ramamoorthy, Differences between amyloid-β aggregation in solution and on the membrane: insights into elucidation of the mechanistic details of Alzheimer's disease, Chem. Soc. Rev. 43 (19) (2014) 6692–6700.
[17] K. Matsuzaki, Aβ-ganglioside interactions in the pathogenesis of Alzheimer's disease, Biochim. Biophys. Acta Biomembr. 2020 (8) (1862) 183233.
[18] S.Y. Cheng, Y. Cao, M. Rouzbehani, K.H. Cheng, Coarse-grained MD simulations reveal beta-amyloid fibrils of various sizes bind to interfacial liquid-ordered and liquid-disordered regions in phase separated lipid rafts with diverse membrane-bound conformational states, Biophys. Chem. 260 (2020) 106355.
[19] B.R. Sahoo, S.J. Cox, A. Ramamoorthy, High-resolution probing of early events in amyloid-β aggregation related to Alzheimer's disease, Chem. Commun. (Camb.) 56 (34) (2020) 4627–4639.
[20] P.H. Nguyen, P. Derreumaux, Structures of the intrinsically disordered Aβ, tau and α-synuclein proteins in aqueous solution from computer simulations, Biophys. Chem. 264 (2020) 106421.
[21] S. Bolognin, L. Messori, D. Drago, C. Gabbiani, L. Cendron, P. Zatta, Aluminum, copper, iron and zinc differentially alter amyloid-Aβ(1-42) aggregation and toxicity, Int. J. Biochem. Cell Biol. 43 (6) (2011) 877–885.
[22] O.V. Bocharova, L. Breydo, V.V. Salnikov, I.V. Baskakov, Copper(II) inhibits in vitro conversion of prion protein into amyloid fibrils, Biochemistry. 44 (18) (2005) 6776–6787.
[23] F. Ricchelli, D. Drago, B. Filippi, G. Tognon, P. Zatta, Aluminum-triggered structural modifications and aggregation of beta-amyloids, Cell. Mol. Life Sci. 62 (15) (2005) 1724–1733.
[24] M.F.M. Sciacca, I. Monaco, C. La Rosa, D. Milardi, The active role of Ca, Chem. Commun. (Camb.) 54 (29) (2018) 3629–3631.
[25] J. Dong, C.S. Atwood, V.E. Anderson, S.L. Siedlak, M.A. Smith, G. Perry, et al., Metal binding and oxidation of amyloid-beta within isolated senile plaque cores: Raman microscopic evidence, Biochemistry. 42 (10) (2003) 2768–2773.
[26] C.D. Syme, R.C. Nadal, S.E. Rigby, J.H. Viles, Copper binding to the amyloid-beta (Abeta) peptide associated with Alzheimer's disease: folding, coordination geometry, pH dependence, stoichiometry, and affinity of Abeta-(1-28): insights from a range of complementary spectroscopic techniques, J. Biol. Chem. 279 (18) (2004) 18169–18177.
[27] V. Minicozzi, F. Stellato, M. Comai, M. Dalla Serra, C. Potrich, W. Meyer-Klaucke, et al., Identifying the minimal copper- and zinc-binding site sequence in amyloid-beta peptides, J. Biol. Chem. 283 (16) (2008) 10784–10792.
[28] B. Sahoo, W. Liang, W. Tang, A. Ramamoorthy, Degradation of Alzheimer's Amyloid-β by a Catalytically Inactive Insulin Degrading Enzyme, (2020).
[29] W.T. Chen, Y.H. Liao, H.M. Yu, I.H. Cheng, Y.R. Chen, Distinct effects of Zn2+, Cu2+, Fe3+, and Al3+ on amyloid-beta stability, oligomerization, and aggregation: amyloid-beta destabilization promotes annular protofibril formation, J. Biol. Chem. 286 (11) (2011) 9646–9656.
[30] C.D. Syme, J.H. Viles, Solution 1H NMR investigation of Zn2+ and Cd2+ binding to amyloid-beta peptide (Abeta) of Alzheimer's disease, Biochim. Biophys. Acta 1764 (2) (2006) 246–256.
[31] P. Adlard, A. Bush, Metals and Alzheimer's disease, J. Alzheimers Dis. 10 (2–3) (2006) 145–163.
[32] A. Budimir, Metal ions, Alzheimer's disease and chelation therapy, Acta Pharma. 61 (1) (2011) 1–14.
[33] X. Liu, H. Cai, H. Huang, Z. Long, Y. Shi, Y. Wang, The prognostic significance of apoptosis-related biological markers in Chinese gastric cancer patients, PLoS One 6 (12) (2011) e29670.
[34] A.S. DeToma, J. Krishnamoorthy, Y. Nam, H.J. Lee, J.R. Brender, A. Kochi, et al., Synthetic flavonoids, aminoisoflavones: interaction and reactivity with metal-free and metal-associated amyloid-β species, Chem. Sci. 5 (12) (2014) 4851–4862.
[35] K.J. Korshavn, M. Jang, Y.J. Kwak, A. Kochi, S. Vertuani, A. Bhunia, et al., Reactivity of metal-free and metal-associated amyloid-β with glycosylated polyphenols and their esterified derivatives, Sci. Rep. 5 (2015) 17842.
[36] H.J. Lee, K.J. Korshavn, Y. Nam, J. Kang, T.J. Paul, R.A. Kerr, et al., Structural and mechanistic insights into development of chemical tools to control individual and inter-related pathological features in Alzheimer's disease, Chemistry. 23 (11) (2017) 2706–2715.
[37] M.W. Beck, J.S. Derrick, J.M. Suh, M. Kim, K.J. Korshavn, R.A. Kerr, et al., Minor structural variations of small molecules tune regulatory activities toward pathological factors in Alzheimer's disease, ChemMedChem. 12 (22) (2017) 1828–1838.
[38] T. Zhang, J. Loschwitz, B. Strodel, L. Nagel-Steger, D. Willbold, Interference with amyloid-β nucleation by transient ligand interaction, Molecules 24 (11) (2019).
[39] G. Olivieri, M. Novakovic, E. Savaskan, F. Meier, G. Baysang, M. Brockhaus, et al., The effects of beta-estradiol on SHSY5Y neuroblastoma cells during heavy metal induced oxidative stress, neurotoxicity and beta-amyloid secretion, Neuroscience. 113 (4) (2002) 849–855.
[40] J.W. Song, B.S. Choi, Mercury induced the accumulation of Amyloid Beta (Aβ) in PC12 cells: the role of production and degradation of Aβ, Toxicol. Res. 29 (4) (2013) 235–240.
[41] C. Suresh, J. Johnson, R. Mohan, C.S. Chetty, Synergistic effects of amyloid peptides and lead on human neuroblastoma cells, Cell. Mol. Biol. Lett. 17 (3) (2012) 408–421.
[42] C. Ha, J. Ryu, C.B. Park, Metal ions differentially influence the aggregation and

deposition of Alzheimer's beta-amyloid on a solid template, Biochemistry. 46 (20) (2007) 6118–6125.
[43] A.S. Pithadia, A. Kochi, M.T. Soper, M.W. Beck, Y. Liu, S. Lee, et al., Reactivity of diphenylpropynone derivatives toward metal-associated amyloid-β species, Inorg. Chem. 51 (23) (2012) 12959–12967.
[44] L. Gerhardsson, T. Lundh, L. Minthon, E. Londos, Metal concentrations in plasma and cerebrospinal fluid in patients with Alzheimer's disease, Dement. Geriatr. Cogn. Disord. 25 (6) (2008) 508–515.
[45] J. Mutter, J. Naumann, C. Sadaghiani, R. Schneider, H. Walach, Alzheimer disease: mercury as pathogenetic factor and apolipoprotein E as a moderator, Neuro Endocrinol. Lett. 25 (5) (2004) 331–339.
[46] J. Mutter, A. Curth, J. Naumann, R. Deth, H. Walach, Does inorganic mercury play a role in Alzheimer's disease? A systematic review and an integrated molecular mechanism, J. Alzheimers Dis. 22 (2) (2010) 357–374.
[47] M. Moschou, C. Papaefthimiou, A. Kagiava, E. Antonopoulou, G. Theophilidis, In vitro assessment of the effects of cadmium and zinc on mammalian nerve fibres, Chemosphere. 71 (10) (2008) 1996–2002.
[48] C. Hock, G. Drasch, S. Golombowski, F. Müller-Spahn, B. Willershausen-Zönnchen, P. Schwarz, et al., Increased blood mercury levels in patients with Alzheimer's disease, J. Neural Transm. (Vienna) 105 (1) (1998) 59–68.
[49] N. Ragunathan, J. Dairou, E. Sanfins, F. Busi, C. Noll, N. Janel, et al., Cadmium alters the biotransformation of carcinogenic aromatic amines by arylamine N-acetyltransferase xenobiotic-metabolizing enzymes: molecular, cellular, and in vivo studies, Environ. Health Perspect. 118 (12) (2010) 1685–1691.
[50] S. Micelli, D. Meleleo, V. Picciarelli, E. Gallucci, Effect of sterols on beta-amyloid peptide (AbetaP 1-40) channel formation and their properties in planar lipid membranes, Biophys. J. 86 (4) (2004) 2231–2237.
[51] P. Müller, D. Rudin, T. Tien, W. Weacott, Reconstitution of cell membrane structure in vitro and its trasformation into an excitable system, Nature. 194 (1962) 979–980.
[52] H.T. Tien, Bilayer Lipid Membrane: Theory and Practice, Marcel Dekker, New York, 1974.
[53] T. Tien, J. Mountz, A. Martinosi, Protein-lipid interaction in bilayer lipid membranes (BLM), The Enzyme of Biological Membranes. NY Plenum, 1977, pp. 139–170.
[54] E. Gallucci, D. Meleleo, S. Micelli, V. Picciarelli, Magainin 2 channel formation in planar lipid membranes: the role of lipid polar groups and ergosterol, Eur. Biophys. J. 32 (1) (2003) 22–32.
[55] V. Stipani, E. Gallucci, S. Micelli, V. Picciarelli, R. Benz, Channel formation by salmon and human calcitonin in black lipid membranes, Biophys. J. 81 (6) (2001) 3332–3338.
[56] S. Micelli, E. Gallucci, D. Meleleo, V. Stipani, V. Picciarelli, Mitochondrial porin incorporation into black lipid membranes: ionic and gating contribution to the total current, Bioelectrochemistry. 57 (2) (2002) 97–106.
[57] N. Arispe, H. Pollard, E. Rojas, Zn2+ interaction with Alzheimer amyloid beta protein calcium channels, Proc. Natl. Acad. Sci. U. S. A. 93 (4) (1996) 1710–1715.
[58] S. Amoroso, A. Gioielli, M. Cataldi, G. Di Renzo, L. Annunziato, In the neuronal cell line SH-SY5Y, oxidative stress-induced free radical overproduction causes cell death without any participation of intracellular Ca(2+) increase, Biochim. Biophys. Acta 1452 (2) (1999) 151–160.
[59] G. Notarachille, F. Arnesano, V. Calò, D. Meleleo, Heavy metals toxicity: effect of cadmium ions on amyloid beta protein 1-42. Possible implications for Alzheimer's disease, Biometals. 27 (2) (2014) 371–388.
[60] D. Meleleo, G. Notarachille, V. Mangini, F. Arnesano, Concentration-dependent effects of mercury and lead on Aβ42: possible implications for Alzheimer's disease, Eur. Biophys. J. 48 (2) (2019) 173–187.
[61] M.A. Lovell, J.D. Robertson, W.J. Teesdale, J.L. Campbell, W.R. Markesbery, Copper, iron and zinc in Alzheimer's disease senile plaques, J. Neurol. Sci. 158 (1) (1998) 47–52.
[62] L.M. Sayre, G. Perry, P.L. Harris, Y. Liu, K.A. Schubert, M.A. Smith, In situ oxidative catalysis by neurofibrillary tangles and senile plaques in Alzheimer's disease: a central role for bound transition metals, J. Neurochem. 74 (1) (2000) 270–279.
[63] X. Li, Y. Lv, S. Yu, H. Zhao, L. Yao, The effect of cadmium on Aβ levels in APP/PS1 transgenic mice, Exp. Ther. Med. 4 (1) (2012) 125–130.
[64] A. Panayi, N. Spyrou, B. Iversen, M. White, P. Part, Determination of cadmium and zinc in Alzheimer's brain tissue using inductively coupled plasma mass spectrometry, J. Neurol. Sci. 195 (1) (2002) 1–10.
[65] M.J. Tamás, S.K. Sharma, S. Ibstedt, T. Jacobson, P. Christen, Heavy metals and metalloids as a cause for protein misfolding and aggregation, Biomolecules. 4 (1) (2014) 252–267.
[66] K. Yano, N. Hirosawa, Y. Sakamoto, H. Katayama, T. Moriguchi, Aggregations of amyloid beta-proteins in the presence of metal ions, Toxicol. Lett. 144 (Supplement 1) (2003) (s134).
[67] S.K.T.S. Wärmländer, N. Österlund, C. Wallin, J. Wu, J. Luo, A. Tiiman, et al., Metal binding to the amyloid-β peptides in the presence of biomembranes: potential mechanisms of cell toxicity, J. Biol. Inorg. Chem. 24 (8) (2019) 1189–1196.
[68] A. Granzotto, M. Suwalsky, P. Zatta, Physiological cholesterol concentration is a neuroprotective factor against β-amyloid and β-amyloid-metal complexes toxicity, J. Inorg. Biochem. 105 (8) (2011) 1066–1072.
[69] D. Meleleo, A. Galliani, G. Notarachille, AβP1-42 incorporation and channel formation in planar lipid membranes: the role of cholesterol and its oxidation products, J. Bioenerg. Biomembr. 45 (4) (2013) 369–381.
[70] N. Arispe, E. Rojas, H. Pollard, Alzheimer disease amyloid beta protein forms calcium channels in bilayer membranes: blockade by tromethamine and aluminum, Proc. Natl. Acad. Sci. U. S. A. 90 (2) (1993) 567–571.
[71] A. Dear, G. Meisl, A. Sacic, T. Michaels, M. Kjaergaard, S. Linse, et al., Identification of on- and off-pathway oligomers in amyloid fibril formation, Chem. Sci. 11 (2020) 6236–6247.
[72] Y. Hirakura, M. Lin, B. Kagan, Alzheimer amyloid abeta1-42 channels: effects of solvent, pH, and Congo red, J. Neurosci. Res. 57 (4) (1999) 458–466.
[73] D.C. Bode, M.D. Baker, J.H. Viles, Ion channel formation by amyloid-β42 oligomers but not amyloid-β40 in cellular membranes, J. Biol. Chem. 292 (4) (2017) 1404–1413.
[74] H. Lin, R. Bhatia, R. Lal, Amyloid beta protein forms ion channels: implications for Alzheimer's disease pathophysiology, FASEB J. 15 (13) (2001) 2433–2444.
[75] S. Scalisi, M.F. Sciacca, G. Zhavnerko, D.M. Grasso, G. Marletta, C. La Rosa, Self-assembling pathway of HiApp fibrils within lipid bilayers, Chembiochem. 11 (13) (2010) 1856–1859.
[76] S. Lesné, M. Koh, L. Kotilinek, R. Kayed, C. Glabe, A. Yang, et al., A specific amyloid-beta protein assembly in the brain impairs memory, Nature. 440 (7082) (2006) 352–357.